

Influence of the pulse energy distribution on the efficiency of ultrasound generation by laser

J.-C. Gonthier, M. Dubois, F. Enguehard, L. Bertrand

► **To cite this version:**

J.-C. Gonthier, M. Dubois, F. Enguehard, L. Bertrand. Influence of the pulse energy distribution on the efficiency of ultrasound generation by laser. *Journal de Physique IV Colloque*, 1994, 04 (C7), pp.C7-685-C7-688. <10.1051/jp4:19947160>. <jpa-00253220>

HAL Id: jpa-00253220

<https://hal.archives-ouvertes.fr/jpa-00253220>

Submitted on 1 Jan 1994

HAL is a multi-disciplinary open access archive for the deposit and dissemination of scientific research documents, whether they are published or not. The documents may come from teaching and research institutions in France or abroad, or from public or private research centers.

L'archive ouverte pluridisciplinaire **HAL**, est destinée au dépôt et à la diffusion de documents scientifiques de niveau recherche, publiés ou non, émanant des établissements d'enseignement et de recherche français ou étrangers, des laboratoires publics ou privés.

Influence of the pulse energy distribution on the efficiency of ultrasound generation by laser

J.-C. Gonthier, M. Dubois, F. Enguehard and L. Bertrand

Ecole Polytechnique de Montréal, Département de Génie Physique, C.P. 6079, Succ. Centre-Ville, Montréal, Québec, Canada, H3C 3A7

Abstract: We have conducted both theoretical and experimental studies of the effect of the energy distribution of the ultrasound generating laser pulse on the amplitude of the longitudinal precursor and on the temporal profile of the displacement for single-point, two-points and line-of-points distributions. These preliminary studies show that the agreement between theory and experiment is generally good and that improvement of the amplitude of the precursor is possible.

1. INTRODUCTION

Laser generation of ultrasound in the thermoelastic regime, especially when coupled to optical detection, has attracted increasing attention lately because of its noncontact and nondestructive nature [1]. Of particular interest is the longitudinal wave thus generated, its first arrival on the opposite side being called the precursor. For some materials the precursor is very small. Thus, it is interesting to try to determine the conditions that will enhance the efficiency of generation of this precursor while still remaining in the thermoelastic regime.

For a given sample of a given material, there are three parameters related to the excitation laser source that may influence the efficiency of the generation: the laser wavelength (and its related optical penetration depth into the material), the duration of the laser pulse and its energy distribution. In this paper, we are interested in the latter parameter. However, determining the optimal surface distribution is a complex problem; moreover, achieving this optimal surface distribution on the experimental may be impossible. Here, we present preliminary experimental and theoretical results obtained with very simple sources: single-point source, two-points source and line-of-points source.

2. EXPERIMENTAL SETUP AND THEORETICAL APPROACH

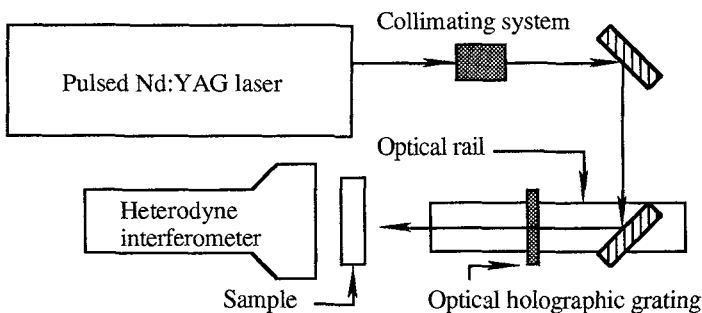


Figure 1: Experimental setup

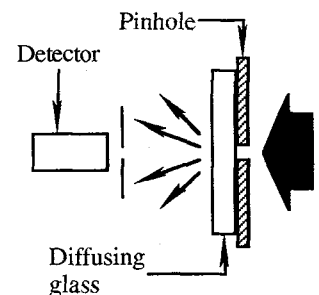


Figure 2: Laser profile measurement system

The excitation source is a pulsed Nd:YAG laser ($\lambda = 1.064 \mu\text{m}$) with a variable repetition rate between 0.1 Hz and 50 Hz. The laser is monomode with a variable pulse energy between 3 and 100 mJ and a pulse duration of 8 ns in the optimal configuration.

The collimating system is composed of two lenses: a concave one and a convex one, the distance between the two lenses being adjustable. This system enables us to produce a spot size on the sample as desired.

The optical holographic grating (fabricated at the Institut National d'Optique (INO) of Québec) is used in the multi-point source experiments. It was designed at INO to divide a laser beam at $1.064 \mu\text{m}$ into seven beams of roughly the same intensities. The distance between the grating and the sample being adjustable, we have the possibility to vary the inter-source spacing at the sample surface.

The sample holder is a five axes stage. It is also used to hold the laser spatial and temporal profile measurement system described in figure 2. This system is composed of a fast photodiode (100 ps risetime) placed behind a $50 \mu\text{m}$ pinhole and a diffusing glass which attenuates the laser pulse. The stage enables us to translate this system normal to the laser beam and thus to measure the laser spatial and temporal profiles.

The detection apparatus is an *Ultra-Optec* OP-35 I/O heterodyne interferometer capable of measuring both in-plane horizontal and normal displacements at a given point. The interferometer is coupled to a *Lecroy* oscilloscope and a data acquisition system.

Numerical simulations were performed using a model developed in our group [2] that calculates the 3-D displacement field over a given meshed surface and a time sequence. The model solves the Christoffel equations coupled with the hyperbolic heat equation using spatial 2-D Fourier and temporal Laplace transformations. The use of these integral transformations allows us to consider any temporal and spatial distributions of the laser source for the ultrasound generation. On the other hand, using Fourier transforms implicitly supposes a periodic energy surface distribution, the period being the meshed surface. Thus, for the single-point source simulations, it was necessary to calculate over a large area in order to avoid superposition with the displacements induced by the virtual sources created by the Fourier transform. This limited the fineness of the mesh. On the other hand, this periodicity was used advantageously to reproduce with a single source a periodic source like a line-of-points distribution. This gave us two ways of simulating multi-point sources: either by simulating one or two points and using the periodicity inherent to the Fourier transform, or by simulating one source and using the superposition theorem.

As for the sample, the experiments were conducted on a BG-18 *Schott* glass. Beside the ease to generate large ultrasonic signals in this glass, it was chosen because its physical constants are well known and readily available, thus giving us the data needed for the simulations. The sample was 3 mm thick and had an optical penetration depth of $103 \mu\text{m}$ at the YAG laser wavelength. It was isotropic, had a longitudinal velocity of 5611 m/s and a transversal velocity of 3346 m/s. Its other physical parameters (density, specific heat, thermal expansion coefficient) used in the simulations acted as a multiplicative constant of the amplitude of the mechanical displacement field.

3. EXPERIMENTAL RESULTS

3.1 Single-point source distribution

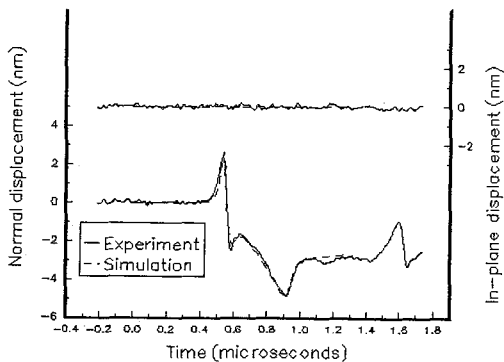


Figure 3: Theoretical and experimental normal and in-plane displacement curves vs time at the epicenter (as expected, the experimental in-plane displacement is zero)

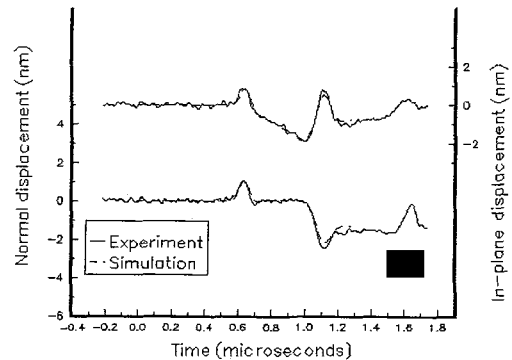


Figure 4: Theoretical and experimental normal and in-plane displacement curves vs time at a distance of 2 mm from the epicenter

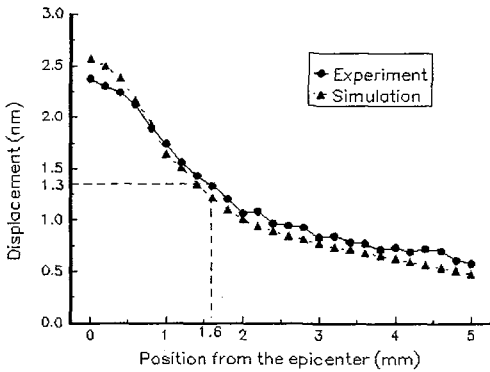


Figure 5: Theoretical and experimental precursor normal displacement amplitude vs distance from the epicenter

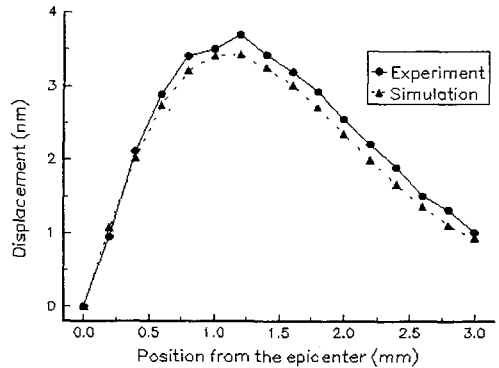


Figure 6: Theoretical and experimental first shear wave arrival in-plane displacement amplitude vs distance from the epicenter

This experiment was performed with the laser beam focused on the sample (the optical holographic grating was removed). The laser spot was Gaussian in shape with a radius at $1/e$ of $340 \mu\text{m}$ and a pulse duration of 33 ns. This latter value is large: we had to lower the output energy of the laser to around 4 mJ per pulse in order not to damage the sample. The simulations were performed with these parameters. The agreement between the calculated displacement curves and the experimentally observed ones was generally good (see figures 3 and 4), except for a slight discrepancy between the amplitudes. We attributed this discrepancy to the misknowledge of the energy absorbed, and we fitted the calculated curves to the experimental ones with a multiplicative constant.

Figures 5 and 6 show respectively the precursor and shear wave displacement amplitude curves versus the distance from the epicenter. From figure 5 one can define an efficiency radius of the point-like source: at a distance greater than 1.6 mm from the epicenter, the normal displacement is less than half the one observed at the epicenter. This value of the efficiency radius determined the spacings we used between the sources in the grating experiments.

3.2 Line-of-points source distribution (3.2 mm spacing)



Figure 7: Spatial distribution of the line-of-points source produced by the optical holographic grating

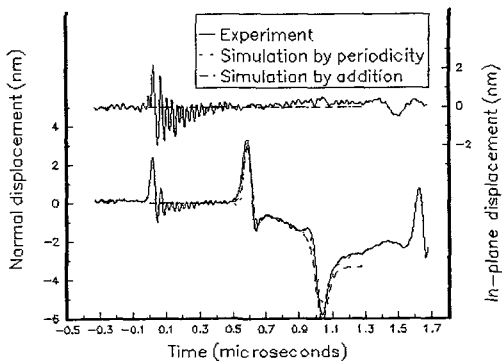


Figure 8: Theoretical and experimental normal and in-plane displacement curves vs time at equal distance from two epicenters (as expected, the experimental in-plane displacement is zero)

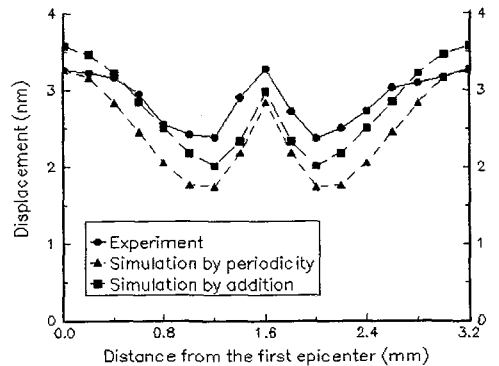


Figure 9: Theoretical and experimental precursor normal displacement amplitude vs distance from one epicenter

In this configuration (the inter-point distance being twice the efficiency radius), it was expected, using the superposition theorem, the precursor amplitude at equal distance from two epicenters to be the same as the one at one epicenter.

Each source had a Gaussian spatial distribution with a radius at $1/e$ of $340 \mu\text{m}$. The energy of each beam was around 4 mJ and the laser pulse duration was 16 ns . Here, we used the two types of simulations discussed earlier: the first one by simulating one point of the grating and using the periodicity created by the Fourier transform (simulation by periodicity), the second one by adding the displacements induced by each source (simulation by addition). Figure 8 compares the normal and in-plane displacements observed experimentally at equal distance from two epicenters to the results of the two types of simulations. Again, the agreement between the three profiles is generally good. On the other hand, problems are encountered with the precursor amplitudes. These problems are essentially of numerical nature; they may also be attributed to misestimated parameters of the experiment (e.g. the laser source distribution). These problems appear again on figure 9. Nevertheless, both theory and experiment show a precursor amplitude peak at equal distance from two epicenters that is due to the simultaneous arrivals of the two longitudinal waves. Moreover, the experimental precursor amplitude at equal distance from the two epicenters is the same as the ones at them, as expected.

3.3 Two-points source distribution (1.6 mm spacing)

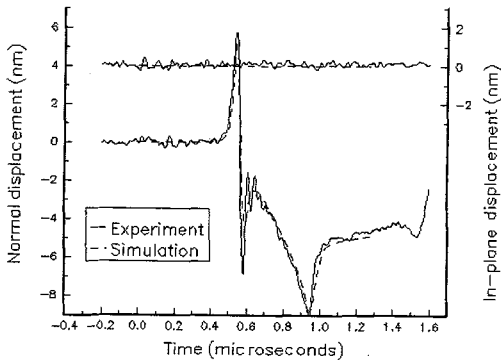


Figure 10: Theoretical and experimental normal and in-plane displacement curves vs time at equal distance from two epicenters (as expected, the experimental in-plane displacement is zero).

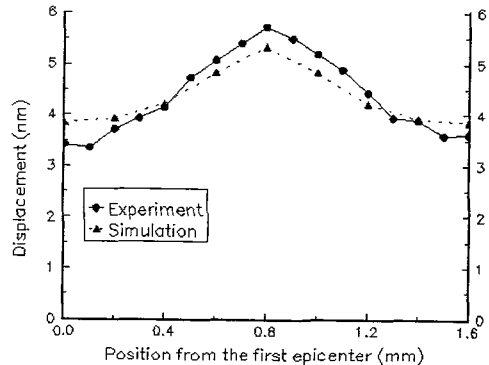


Figure 11: Theoretical and experimental precursor normal displacement amplitude vs distance from one epicenter

In this configuration (the inter-point distance being less than twice the efficiency radius), it was expected the precursor amplitude at equal distance from two epicenters to be greater than the one at one epicenter.

For this experiment, the use of the simulation by periodicity was problematic and was thus abandoned. Because of the short inter-source distance, this simulation created sources that did not exist in the experiment. Since this left us with only the simulation by addition, it was better to use two sources out of seven in order not to cumulate errors.

The remarks we made for figures 8 and 9 still apply for figures 10 and 11. As expected, theory and experiment show an improvement of the precursor amplitude at equal distance from the two epicenters.

4. CONCLUSION

These preliminary studies have shown that improvement of the precursor amplitude in the thermoelastic regime is possible with the help of an optical holographic grating. A single source with the total energy used in the multi-point source experiment would obviously generate larger precursors, but with the risk of going beyond the damage threshold of the material.

References:

- [1] Monchalain J.P., *Review of Progress in Quantitative Nondestructive Evaluation* **12** (1993), 495-506
- [2] Dubois M., Enguehard F., Bertrand L., Choquet M. and Monchalain J.P., *Appl. Phys. Lett.* **64**(5) (1994), to be published.